

In Situ Kinase Profiling Reveals Functionally Relevant Properties of Native Kinases

Matthew P. Patricelli,^{1,*} Tyzoon K. Nomanbhoy,¹ Jiangyue Wu,¹ Heidi Brown,¹ David Zhou,¹ Jianming Zhang,² Subadhra Jagannathan,¹ Arwin Aban,¹ Eric Okerberg,¹ Chris Herring,¹ Brian Nordin,¹ Helge Weisig,¹ Qingkai Yang,³ Jiing-Dwan Lee,³ Nathanael S. Gray,² and John W. Kozarich¹

¹ActivX Biosciences, La Jolla, CA 92037, USA

²Dana Farber Cancer Institute, Departments of Cancer Biology, and Biological Chemistry and Molecular Pharmacology, Harvard Medical School, Boston, MA 02115, USA

³Department of Immunology, The Scripps Research Institute, La Jolla, CA, 92037, USA

*Correspondence: mattp@activx.com

DOI 10.1016/j.chembiol.2011.04.011

SUMMARY

Protein kinases are intensely studied mediators of cellular signaling, yet important questions remain regarding their regulation and *in vivo* properties. Here, we use a probe-based chemoproteomics platform to profile several well studied kinase inhibitors against >200 kinases in native cell proteomes and reveal biological targets for some of these inhibitors. Several striking differences were identified between native and recombinant kinase inhibitory profiles, in particular, for the Raf kinases. The native kinase binding profiles presented here closely mirror the cellular activity of these inhibitors, even when the inhibition profiles differ dramatically from recombinant assay results. Additionally, Raf activation events could be detected on live cell treatment with inhibitors. These studies highlight the complexities of protein kinase behavior in the cellular context and demonstrate that profiling with only recombinant/purified enzymes can be misleading.

INTRODUCTION

Protein kinases are found in all forms of life and are the largest enzyme family in mammals (Manning et al., 2002). Nearly all signal transduction pathways rely on protein kinase cascades that tightly regulate processes such as cell division, differentiation, activation, and migration. Efforts to generate selective and efficacious kinase-targeted drugs resulted in the first clinically approved kinase inhibitor, Gleevec, in 2001 for the treatment of chronic myelogenous leukemia (Cohen et al., 2002). The success of Gleevec and the promise of protein kinases as therapeutic targets in other disease areas have rapidly expanded pharmaceutical research efforts on kinase inhibitors and supported a growing industry of kinase assay methodologies and research tools (Cohen, 2002; Noble et al., 2004).

Most kinase inhibitors that have been approved or are currently in clinical development are competitive inhibitors of ATP binding. However, >500 human protein kinases are known

and they share high structural conservation in the ATP-binding site. Therefore, achieving a significant degree of target selectivity via the ATP binding site is an imposing problem (Toledo et al., 1999; Garcia-Echeverria et al., 2000). This challenge has been met for several compounds, such as lapatinib, which shows impressive selectivity for epidermal growth factor receptor (EGFR) (Karaman et al., 2008). Nonetheless, it should be noted that the vast majority of ATP-competitive kinase inhibitor have only been approved for the treatment of cancer, where otherwise unacceptable toxicities can often be managed.

Rapid and cost-effective assays for nearly every human protein kinase are now available due to the combined efforts of academic and industrial research. Many different assay methodologies exist and most of these rely on recombinant expression and purification of the kinase of interest or a catalytically active fragment. The biological functions of most kinases, however, are regulated by dynamic, posttranslational mechanisms in cells. These regulatory events have also been shown to require kinases to exist in physical complexes with their substrates and/or partner kinases that allow for spatial and temporal regulation (Garrington and Johnson, 1999; Newton, 2001). Although kinase assay methodologies using recombinant enzymes are clearly valuable tools, these methods are not capable of capturing the complexity of kinase function and regulation seen in native biological systems. Thus, most kinase-directed medicinal chemistry efforts instead rely on cellular assays that report on the kinase of interest as a primary means of deducing structure-activity relationships.

Chemical proteomics (chemoproteomic) methodologies have been developed recently for evaluating small-molecule binding to protein kinases in native systems, such as in cell or tissue lysates. Two reported methods rely on the attachment of kinase inhibitors to solid supports (Godl et al., 2003; Bantscheff et al., 2007; Sharma et al., 2009). The methods described by Bantscheff et al. (2007) and Sharma et al. (2009) use broadly-selective kinase inhibitors tethered to a solid support to capture and evaluate more than 200 kinases from cell lysates. These kinases can be competed off the support through the addition of select inhibitors and thus selectivity can be evaluated. A similar method was described by Godl et al. (2003) that involves the attachment of a selected inhibitor to a solid support (typically through biotin attachment), permitting affinity enrichment of the kinase targets of the compound. Using both

of the above methods, quantitative inhibitor binding information can be obtained through the use of isotopic labeling strategies (Bantscheff et al., 2007; Sharma et al., 2009). We have reported an alternative method for profiling kinases in native systems, termed KiNativ, that utilizes soluble chemical probes comprised of ATP and ADP linked to biotin through an acyl-phosphate bond (Patricelli et al., 2007). These probes covalently modify conserved lysine residues in the ATP binding site of essentially all protein kinases in addition to labeling active-site lysine residues in other ATP binding proteins. When coupled with a mass spectrometry (MS) based analysis platform, these probes enable the detection and characterization of >300 endogenous protein and lipid kinases, as well as hundreds of other nucleotide-dependent enzymes. We have also previously described the detection of ~60 kinases from a single cell line, with ~40 of these exhibiting adequate signal for quantification (Patricelli et al., 2007). In this study, we present several fundamental improvements to the platform that have enabled efficient measurement of binding constants for small-molecules against >150 protein kinases in parallel, using only a single cell line, and >200 total kinases from two cell lines. Binding constants are presented for ATP as well as several research and clinical-stage kinase inhibitors. Notably, we reveal that kinases can show strikingly different inhibitor sensitivity profiles in native versus recombinant systems and demonstrate that the cellular efficacy of these kinase inhibitors is accurately predicted by KiNativ.

RESULTS

Rationale for and Development of Kinase-Focused MS “Target Lists”

We previously found that biotin-tagged acyl-phosphates of ATP and ADP are capable of acylating the conserved active site lysines in a broad range of known human protein and lipid kinases as well as other ATP-dependent enzymes (Figures 1A and 1B) (Patricelli et al., 2007). The reaction of these probes with their target kinases can be quantitatively monitored by digesting the treated cell-lysates with a protease (trypsin), affinity-enriching the biotinylated peptides on streptavidin beads, and analyzing the resulting labeled peptides by liquid chromatography-tandem MS (Figure 1C). Although our original protocols were adequate for illustrating the usefulness of acyl-phosphates as kinase affinity probes, further optimization was required to maximize the scope and utility of this method.

The most critical issues for the optimization of KiNativ were to improve the sensitivity and accuracy of quantification. Our initial protocols were developed to analyze biotin-labeled peptides in “data-dependent” mode on an ion-trap mass spectrometer. In this acquisition mode, the mass spectrometer requires the signal strength in the parent ion (MS) spectrum to be in the top 10–20 ions before a fragment spectrum is collected. With the acyl-phosphate probes used in these studies as many as 1000 different probe-labeled peptides can be detected in a given sample and many of the active site protein kinase peptides are present at very low levels relative to other labeled ATPases. These factors contributed to poor reproducibility and sensitivity in the data-dependent MS mode, particularly for low abundance species in complex mixtures. To overcome these limitations, we

developed a “targeted” MS approach on a linear ion trap mass spectrometer, whereby the instrument is preprogrammed to collect MS/MS data on known kinase peptide ions at specified times (Figure 1D). This approach is analogous to multiple-reaction-monitoring (MRM) using triple-quadrupole mass spectrometers and has recently garnered interest in its application to proteomics experiments using ion trap mass spectrometers (Schmidt et al., 2009; Domon and Aebersold, 2010).

This targeted approach requires a priori knowledge of the kinase proteins expressed in the sample (cell lysate) of interest, which we obtained by performing exhaustive data dependent analyses with both ATP and ADP acyl-phosphate probes. Analysis of HL60 and PC3 cell lysates yielded data on approximately 160 kinases per cell line and ~220 kinases in total. Based on these data sets, parent ions corresponding to each kinase were selected for targeting and assembled into time-segmented target lists specific for each probe-proteome combination. It should be noted that scan rate limitations for the MS instrumentation used here limited the total number of ions targeted in a given run. Therefore, a subset of labeled proteins (e.g., kinases) was selected such that a coherent data set of related enzymes would result. Similar target lists for other probe-labeled enzyme families are currently under development.

Data collected using the kinase target lists described above was analyzed by extracting characteristic fragment ions for each kinase peptide. Using this approach, we found that the signal/noise ratio of the summed fragment ion traces from the targeted MS/MS spectra were typically ~50-fold higher than the signal/noise ratio of the corresponding parent ion chromatograms in the MS scans (only parent ion/MS data is available for signal quantitation in data-dependent MS runs) (Figure 1D). In many cases, robust, clean peaks could be extracted from MS/MS spectra when no peak could be detected in the MS scans. Using a single proteome and either the ATP or ADP probe, >100 kinases could be detected with sufficient signal to allow for robust quantitation. Both probes are used in most studies due to slight variations in the coverage and labeling efficiency between probes (Patricelli et al., 2007). Overall, this targeted method dramatically improved the detection and quantitation of acylphosphate probe-labeled kinases.

Profiling ATP and Kinase Inhibitors with KiNativ

One of our major goals was to accurately determine binding constants for kinase inhibitors against native kinases. In any competitive, activity-based profiling method, a critical consideration is the effect of probe binding and irreversible labeling kinetics on the observed inhibition by a reversible inhibitor (Leung et al., 2003). Observed IC_{50} values can be dramatically shifted from true K_d values if the probe concentration is too high or the reaction time is too long. We addressed this potential complication by determining IC_{50} values for ATP binding under both high (20 μ M) and low (1 μ M) probe labeling conditions. The results of this analysis allowed for the selection of a probe concentration (5 μ M) and labeling time (10 min) where >90% of the kinase targets showed a <3-fold shift between ATP IC_{50} and the apparent K_d (K_d^{app}) value. Additionally, for kinases showing probe-related IC_{50} shifts, the magnitude of the shift was determined so that the IC_{50} could be corrected to yield an accurate K_d^{app} value (see Experimental Procedures) It is

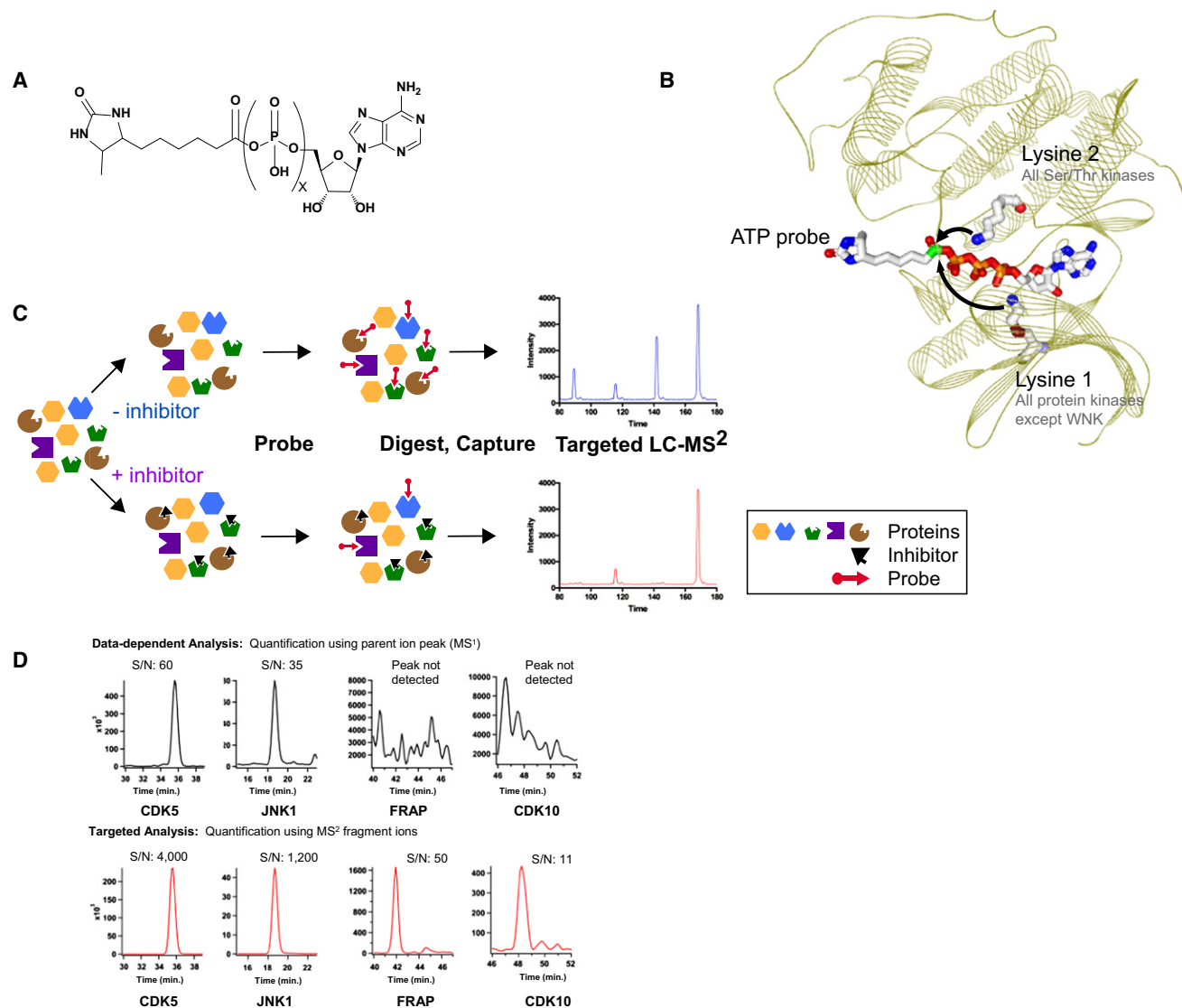


Figure 1. The KiNativ Method

(A) Chemical structure of the acylphosphate probe.

(B) Schematic of the KiNativ method. Protein lysates are treated with an inhibitor followed by addition of the desthiobiotinylated acylphosphate-nucleotide probe. After a tryptic digest and streptavidin enrichment, the probe labeled peptides are characterized and quantified using a targeted LC-MS² strategy.

(C) Model of an acylphosphate probe bound in the active site of CDK2 (PDB ID 1HCK). Conserved, catalytic lysine residues are illustrated.

(D) Signal enhancement through targeted LC-MS² analysis. Signals from MS¹ (or parent) ion signals typically used for quantification in nontargeted runs (top) are compared to extracted MS/MS ions from a targeted LC-MS² run (bottom).

important to note that this K_d^{app} value may differ from a K_d value obtained using purified recombinant kinase binding or activity assays due to a variety of assay specific factors including differences in endogenous/full length versus truncated kinase constructs, conformation and/or activation states, protein-protein interactions, etc. It is also likely that kinase conformations and activation states in both recombinant enzyme preparations and cell lysates are heterogeneous. The possibility therefore exists that the differential sensitivity of various assays to subpopulations of enzyme may skew the results of the ensemble average or mask the response of subpopulations that do not significantly contribute to the measured signal. However, the

K_d^{app} determined here should represent the occupancy of the probe accessible enzyme population within a biological background.

Table 1 shows selected results from the profiling of ATP, staurosporine, dasatinib (Sprycel), imatinib (Gleevec), erlotinib (Tarceva), BIRB796, and sorafenib (Nexavar) in HL60 and PC3 lysates. These compounds are all ATP competitive kinase inhibitors and represent examples of both Type I (DFG-in) and Type II (DFG-out) binding preferences (Liu and Gray, 2006). The complete data set is presented in Table S1 available online. It is important to note that, before addition of either exogenous ATP or an inhibitor, the cell lysates are subjected to

Table 1. Inhibition Profiles for Reference Compounds and Clinically Relevant Kinase Inhibitors

Kinase name	ATP K _d ^{app}	Staurosporine	Dasatinib	Erlotinib	BIRB796	Sorafenib	Imatinib
ABL1/2	5.2	13	0.0067, 0.0034	>10	>10	>10	0.21, 0.15
ACK	22	0.062	0.033	>10	>10	>10	>10
AurA/B/C	9.5	0.076	>10	7.4	>10	>10	>10
AurB	31	0.03, 0.012	>10, >4	6.4, 2.6	>10, >4	>10, >4	>10, >4
BRAF	6.1	>10	3.2	>10	>10	>10	>10
BTK	86	0.91	0.013	>10	>10	>10	>10
CDK5	13	0.64	>10	>10	>10	>10	10
CDK8/11	19	2.2	>10	>10	>10	>10	11
CSK	17	2.9, 2.4	0.015, 0.012	>10	>10	>10	>10
EGFR	18	>10	4.7, 4.1	0.3, 0.19	>10	>10	>10
EphA1	1.7	4.3	0.022	>10	>10	>10	>10
EphA2	22	11	0.017	>10	>10	>10	>10
EphB2	5.2	10	0.014	>10	>10	>10	>10
EphB4	8.5	>10	0.0028	5.2	>10	>10	>10
FGR	2.6	0.92, 0.37	0.0068, 0.0027	>10, >4	>10, >4	>10, >4	>10, >4
FYN	ND	0.27, ND	ND	5.8, ND	ND	>10, ND	ND
GCK	26	0.1	5	>10	>10	>10	>10
GCN2	92	1.3, 1.1	>10	0.76, 0.6	>10	>10	>10
HCK	10	0.43	0.015	>10	>10	>10	>10
ILK	57	>10	0.24	1.1	>10	>10	>10
IRAK3	360	0.012	10	>10	>10	>10	ND
JAK1 (Domain 2)	1.8	0.21, 0.051	5.3, 1.3	>10, >2.5	10, >2.5	>10, >2.5	>10, >2.5
JNK1/2/3	19	9.2	>10	>10	0.087	>10	8.6
JNK2	ND	3.1	>10	>10	0.029	>10	5.3
KHS1	9.6	0.12	0.4	>10	>10	>10	>10
KHS1/2	7.8	0.23	2.2	>10	>10	>10	>10
LOK	12	0.012	10	1.2	1	5.3	>10
LYN	1	0.41	0.0031	>10	>10	>10	>10
MAP2K1	8.1	0.49, 0.2	10, 4	>10, >4	>10, >4	ND	>10, >4
MAP2K5	2.6	2.6, 1.4	0.058, 0.037	10	>10	>10	>10
MAP3K1	64	10	0.49	0.63	>10	0.82	>10
MAP3K2	7.9	1	6.5	>10	>10	>10	>10
MAP3K4	20	>10	0.51	>10	>10	>10	>10
MET	74	0.63, 0.67	>10	3.5, 2.4	>10	>10	>10
MINK,HGK,TNIK	7.6	0.11	>10	>10	1.1	>10	>10
MLKL	150	>10	3.2	>10	>10	>10	>10
p38a	570	>10	0.77	>10	0.19	2.4	>10
p38d/g	300	1.3	>10	>10	0.45	>10	>10
PIK3C3	97	>10	>10	>10	>10	>10	9.5
PIP5K2c	63	>10	>10	3.7	>10	>10	1.5
PIP5K3	7	10	>10	>10	>10	>10	4.2
PYK2	70	0.2	>10	>10	9	>10	>10
QSK	20	0.12	0.39	>10	>10	>10	>10
SLK	3.8	0.0091	>10	0.58	>10	>10	>10
SRC	9.8	0.89	0.0033	>10	>10	>10	>10
STLK5	54	>10	0.64, 0.21	>10	>10	>10	>10
SYK	3.2	0.045	10	>10	>10	>10	>10
TAO2	1.1	0.71, 0.46	>10	>10	>10	7.1, 2.8	>10
TEC	ND	>10, ND	0.55, <0.079	>10, ND	10, ND	>10, ND	>10, ND

Table 1. Continued

Kinase name	ATP K_d^{app}	Staurosporine	Dasatinib	Erlotinib	BIRB796	Sorafenib	Imatinib
YES	31	1.1	0.0032	>10	>10	>10	>10
ZAK	19	10	0.1445	>10	5.4	0.103	>10

Selected results are illustrated from the profiling of ATP, staurosporine, dasatinib (Sprycel), imatinib (Gleevec), erlotinib (Tarceva), BIRB796, and sorafenib (Nexavar) in HL60 and PC3 proteomes. Data are shown where significant inhibition with the clinically relevant kinase inhibitors was observed. The data was generated with a 15-min preincubation. Approximately 220 kinases were evaluated for inhibitory activity. ND, not determined. See also Table S1 and Figures S1–S3.

rapid gel-filtration to remove endogenous ATP and other competing factors. Approximately 220 kinases were profiled in total, with >400 total data points per compound when redundancies between cell/probe target lists are considered (complete table in Table S1). Internal consistency between redundant data points was excellent with most cases showing IC_{50}/K_d^{app} values within a 2-fold margin. It should be noted that although the data presented in Table 1 illustrate the K_d^{app} for the enzymes profiled, all other data presented in this article will be presented as an IC_{50} values (as indicated). For the vast majority of enzyme/probe combinations the relative shift between the IC_{50} and K_d^{app} is <3, therefore the IC_{50} data are close approximations of the K_d^{app} .

Several efforts were made to further validate the method and resulting IC_{50} values. First, to demonstrate the linearity of signal response, a recombinant kinase (ErbB2) was spiked into a background proteome absent of the spiked kinase (HL60 lysate) and the integrated signal was measured (Figure S1A). As expected, the integrated signal response was linear down to a signal/noise ratio of 3. Second, to verify that the measured IC_{50} values are representative of the actual K_d^{app} values, we evaluated the effect of probe concentration on staurosporine IC_{50} values in a second cell line (A375 cell lysate) (Figure S1B and Table S2). As predicted, the majority of the data did not demonstrate a >3-fold shift in IC_{50} value. We further demonstrated that the IC_{50} values are independent of protein concentration by comparing IC_{50} values obtained at two protein concentrations (Figure S1C). Finally, measured IC_{50} values for staurosporine were compared between multiple cell lines and probe types and were found to be in excellent agreement with one another (Figures S1D and S1E). Replicate data from profiling a Raf inhibitor, PLX4720, also showed excellent

agreement between measurements (Figure S1F and Table S3). Overall, these data support that the IC_{50} values presented here are typically reproducible within a 2-fold margin.

For broad-spectrum kinase inhibitors such as staurosporine, comprehensive data are available from recombinant enzyme assays and could be used as another form of validation. Overall, K_d^{app} values for staurosporine measured by the probe-based assay, were on the order of 10–20-fold weaker than K_d values determined for purified recombinant kinases in activity or binding assays (Figure S2). However, if this general shift is taken into account, the correlation of relative potency between the methods is reasonably robust. It is interesting to note that the reported in vivo potency of staurosporine against PMA-induced PKCa signaling (Table 2) (Winkler et al., 1988), is essentially identical to the K_d^{app} value and is 14-fold higher than the staurosporine IC_{50} determined in a recombinant kinase assay (www.invitrogen.com). Moreover, a robust correlation between the K_d^{app} and cellular efficacy was observed for those inhibitors where the cellular efficacy could be corroborated (Table 2).

Erlotinib Selectively Inhibits Membrane-Bound over Detergent-Solubilized EGFR

In our initial evaluation of erlotinib inhibitory activity, it was observed that the K_d^{app} for erlotinib against EGFR in PC3 cells (0.19 μ M) (Figure S3) was considerably higher than the reported literature values for cellular EGFR potency (4–20 nM) (Carey et al., 2006; Schiffer et al., 2007). To further investigate this observation, we explored solubilized and intact membrane samples from resting and EGF stimulated MDA-MB-231 cells that express EGFR at higher levels than PC3 cells (Table S4). Additionally, a lower probe dose (1 μ M) was used because

Table 2. Correlation between Cellular Efficacy and KiNativ Measured IC_{50} Values

	Target	Cellular Efficacy EC_{50} (nM)	KiNativ IC_{50} (nM)	Cellular Assay Type	Reference
Dasatinib	Abl1/2	1.5	3.4	Abl autophosphorylation	Manley et al. (2005)
Dasatinib	SRC	4.3	3.3	SRC autophosphorylation	Du et al.(2009)
Imatinib	Abl1/2	200	150	Abl autophosphorylation	Manley et al. (2005)
BIRB796	p38	30	11 ^a	MapKap-K2 phosphorylation	Kuma et al. (2005)
BIRB796	JNK	1000	87	c-Jun Phosphorylation	Kuma et al. (2005)
SB203580	p38	280	85	TNF- α release	Mihara et al. (2005)
Erlotinib	EGFR	24.5	18	EGFR autophosphorylation	Carey et al. (2006)
Staurosporine	PKC	30	27	Ca ⁺² mobilization	Winkler et al. (1988)

The type of cellular assay from each reference is listed. When possible, references were selected that demonstrated the most direct measure of inhibitor activity rather than downstream cellular response (e.g., cell viability or proliferation).

^a The value used is calculated from the 4-hr preincubation data.

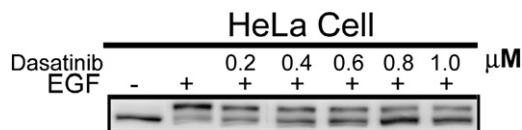


Figure 2. Dasatinib Inhibits MAP2K5

HeLa cells were treated with varying concentrations of dasatinib for 1 hr before treatment with EGF. Cells lysates were analyzed by a mobility shift western blot for phosphorylation of ERK5, a substrate of MAP2K5. See also Figure S4.

EGFR was found to show a ~3-fold shift of IC_{50} from K_d^{app} at the standard 5 μ M probe dose. Consistent with the data collected in detergent solubilized PC3 cell lysates, 0.1 μ M erlotinib did not significantly inhibit EGFR in detergent solubilized lysates from MDA-MB-231 cells. In contrast, EGFR from intact membrane preparations of MDA-MB-231 cells was inhibited and a slight increase in potency was observed after 5 min cellular stimulation with 500 ng/ml EGF (Table S4). Thus, when the conditions of cellular efficacy are closely replicated (i.e., intact membranes and activated EGFR), the potency of erlotinib against EGFR determined here closely matches reported cellular efficacy (Table 2).

Dasatinib Is an Inhibitor of MAP2K5

Dasatinib is a clinically approved drug that is a potent inhibitor of a large number of tyrosine kinases and shows a predilection for kinases possessing a “gatekeeper” threonine residue (Hantschel et al., 2007). The kinase targets of dasatinib have been evaluated using recombinant enzyme panels, phage display methods, and chemical proteomic approaches (Bantscheff et al., 2007; Karaman et al., 2008). In addition to confirming many of the known targets of dasatinib, our profiles identified MAP2K5 as an unreported, potent target of dasatinib ($K_d^{app} = 37$ nM) (Figure S4). MAP2K5 is unusual among the MAP2K kinases in that it forms a signaling complex with ERK5. To test whether the observed binding of dasatinib to MAP2K5 would translate into cellular inhibition of ERK5 phosphorylation, EGF-stimulated HeLa cells were treated with various concentrations of dasatinib and the level of ERK5 phosphorylation was quantified (Figure 2). For thoroughness, an additional cell line (A549) was evaluated to corroborate MAP2K5 as a target of dasatinib and the inhibition of MAP2K5 was confirmed (Figure S4D). The HeLa cell experiment demonstrated that dasatinib inhibited phosphorylation of ERK5 with a cellular EC_{50} of 0.56 μ M and further illustrates that KiNativ profiling can identify new kinase-inhibitor interactions, even for inhibitors that have been subject to extensive profiling by other approaches. The most comprehensive published profile of dasatinib did not cover MAP2K5 despite the fact that >300 protein kinases were profiled (Karaman et al., 2008). Additionally, of the MAP2K isoforms present in that study (MAP2K1,2,3,4,6), only MAP2K1 and MAP2K2 were weakly inhibited by dasatinib. Interestingly, the only literature report we have found showing any affinity of dasatinib for Map2K5 was from an alternate chemical proteomics approach (Bantscheff et al., 2007) where an IC_{50} value of 1.2 μ M was observed. Importantly, later work has shown that the IC_{50} values from this study were systematically affected by assay properties (similar to the kinetic issues possible with our probes), and thus may

not have reflected true binding potencies (Sharma et al., 2009). Further, the relatively poor affinity observed in the study by Bantscheff et al. (2007) did not suggest Map2K5 as a significant or noteworthy target relative to other targets of the compounds.

Comparison of Native and Recombinant Raf Kinases

A surprising discovery from the inhibitor profiles (Table 1) was the lack of B-Raf inhibition by sorafenib. Sorafenib was initially developed as a Raf kinase inhibitor and consistently showed good potency against Raf kinases in recombinant assays (Wilhelm et al., 2004). To further investigate the possible differences between native and recombinant Raf kinases we selected two well-studied compounds, GW5074 (Lackey et al., 2000) and SB203580 (Cuenda et al., 1995), with reported Raf activities as well as two more recently developed B-Raf inhibitors, PLX4720 (Tsai et al., 2008) and SB590885 (Takle et al., 2006). Chemical structures for the Raf inhibitors are presented in Figure S5. GW5074 has also widely been reported as a Raf-1 (C-Raf) selective inhibitor, however, early studies did not assess potency of this compound against A-Raf or B-Raf. Recent reports have shown that GW5074 has potent activity against B-Raf in recombinant kinase assays (Kupcho et al., 2008). SB203580 is a well studied, relatively selective inhibitor of p38 kinases; however, recombinant profiling efforts have found moderate B-Raf inhibition (Karaman et al., 2008). PLX4720 and SB890885 have both been shown to exert potent B-Raf inhibition in recombinant and cellular assays. For all five compounds, we determined binding to recombinant and native B-Raf (Table 3, columns 2 and 4), V600E-B-Raf (Table 3, columns 3 and 5), Raf-1 (Table 4, column 2 and 3), and A-Raf (Table 4, column 4). KiNativ evaluation of native wild-type (WT) B-Raf was determined in HL60 cells, whereas V600E-B-Raf, Raf-1, and A-Raf were monitored in the A375 melanoma cell line that expresses the V600E-B-Raf mutation. All Raf probe labeling experiments were performed using the ATP-based probe and example data illustrating PLX4720 inhibition of the Raf kinases are presented in Figure S6. Recombinant Raf assays were performed by monitoring recombinant MAP2K1 phosphorylation at S218/222 by western blotting. Cellular activity of the five compounds was determined using both cellular proliferation inhibition assays (Table 3, column 7), and phospho-ERK1/2 inhibition assays (Figure S7) in the A375 melanoma cell line.

The inhibitor sensitivity profiles measured in our recombinant Raf assays agreed well with reported literature values. However, the ability of these compounds to inhibit ERK1/2 phosphorylation and proliferation in A375 cells was not well predicted by the in vitro/recombinant kinase assays. For example, GW5074 and SB590885 exhibited nearly identical potencies against recombinant V600E-B-Raf (24 nM and 43 nM, respectively), however, GW5074 was >300-fold weaker ($EC_{50} > 10$ μ M) in the cellular proliferation assay than SB590885 ($EC_{50} = 0.03$ μ M). SB590885 was also a dramatically more potent inhibitor of ERK1/2 phosphorylation in vivo than GW5074. In contrast to the recombinant assay results, the in vivo p-ERK1/2 inhibition and antiproliferative activity of the Raf inhibitors was highly consistent with their behavior against native V600E-B-Raf measured here. For example, the dramatic cellular potency difference observed for SB590885 and GW5074 nicely matched

Table 3. Inhibitory Activity of Raf Inhibitors Evaluated against Multiple B-Raf Isoforms

Assay Format	In Vitro MAP2K1 Phos.		KiNativ		KiNativ	Cellular Proliferation
	Recombinant		HL60	A375	Recombinant	A375
Enzyme Source	WT-B-Raf	V600E-B-Raf	WT-B-Raf	V600E-B-Raf	V600E-B-Raf	V600E-B-Raf
Sorafenib	0.63	0.18	>10	>10	ND	4
SB203580	0.69	0.309	>10	4.7	ND	>10
GW5074	0.011	0.024	>10	2.6	0.16	>10
SB590885	0.004	0.043	0.1	0.006	ND	0.03
PLX4720	0.053	0.09	0.05	0.008	1.3	0.03

Several Raf inhibitors were evaluated in an in vitro phosphorylation assay using recombinant B-Raf, by KiNativ using both recombinant B-Raf and endogenously expressed enzyme (both wild-type and V600E isoforms), and in a cellular proliferation assay using endogenously expressed V600E-B-Raf. ND, not determined. See also Figure S4., Figure S5, Table S5, and Table S6.

the binding of these compounds to native V600E-B-Raf (IC_{50} values of 2.6 μ M and 0.006 μ M for GW5074 and SB590885, respectively). Overall, the native kinase binding affinity determined in KiNativ for various Raf kinase inhibitors was consistent with the cellular antiproliferative activity and p-ERK1/2 inhibition for all compounds tested.

To investigate the possible reasons for the dramatic difference between V600E-B-Raf binding and the recombinant kinase assay, we evaluated the binding of GW5074 and PLX4720 to recombinant V600E-B-Raf using our probe-based assay (Table 3, column 6). GW5074 and PLX4720 showed similar relative binding affinities compared to the MAP2K1 phosphorylation assay, with GW5074 being 5–10-fold more potent than PLX4720 against recombinant V600E B-Raf in both assay formats. Thus, the difference in behavior of the recombinant and native B-Raf assays appears to reflect differences in the behavior of the recombinant B-Raf protein, rather than only differences between the assays themselves.

Similar to what was found for WT and V600E-B-Raf, we found striking differences in the potencies of the five compounds against native versus recombinant Raf-1. None of the compounds tested appeared to be potent Raf-1 inhibitors based on KiNativ measurement. A-Raf binding measurements revealed that PLX4720 was unique among the compounds tested in being a potent inhibitor of A-Raf. No recombinant assays have been reported for A-Raf, so comparisons with in vitro assay systems

could not be made. Select data from the profiling of Raf inhibitors are presented in Table S5 and the complete data set is presented in Table S6.

Complex Behavior of Raf Kinase Signaling Pathways

To further explore the behavior of Raf kinase inhibitors and their effects in cellular systems, we treated living A375 cells with these compounds for 30 min and then profiled lysates from treated cells using the KiNativ platform (Figure 3). Before probe labeling with the ATP-based probe, the lysates were gel-filtered to remove any compound that had entered the cells. In parallel experiments, non-gel-filtered lysates were analyzed and the inhibition profiles observed were entirely consistent with the targets observed for these compounds in lysate profiling experiments described above (data not shown).

Surprisingly, significant increases in Raf-1 probe-labeling were observed in cells treated with SB590885, SB203580, and PLX4720. PLX4720 also caused a dramatic increase in A-Raf labeling despite the fact that PLX4720 is a potent inhibitor of A-Raf. We believe that this paradoxical finding may be due to a change in conformation of A-Raf that decreases its affinity for PLX4720, however, the precise mechanism is still under investigation. Due to the short cellular treatment time (30 min), changes in transcription seemed an unlikely basis for the increased probe-labeling signals. Moreover, the fact that the inhibitors were removed before probe labeling indicates that significant, lasting alterations to the enzyme are induced through interaction with the inhibitor. In light of this and other work (Hatzivassiliou et al., 2010; Poulikakos et al., 2010), the increased labeling of A-Raf and Raf-1 is most likely due to changes in the conformation of these kinases leading to either increased affinity for ATP or a more optimal positioning of their catalytic lysine residues for probe labeling. These findings demonstrate that KiNativ can detect inhibitor induced conformational changes in the ATP binding site of native kinases within a biological context. They also suggest that the platform could be used to distinguish inhibitors based on their specific effects on complex kinase signaling pathways.

DISCUSSION

The results presented here represent the most comprehensive analysis of the binding properties of native kinase ATP sites

Table 4. Inhibitory Activity of Raf Inhibitors Against Raf-1 (C-Raf) and A-Raf

Assay Format	In Vitro MAP2K1 Phos.	KiNativ	
		A375	A375
Enzyme Source	Recombinant	Raf-1	A-Raf
Kinase	Raf-1	Raf-1	A-Raf
Sorafenib	0.027	>10	>10
SB203580	1.8	>10	>10
GW5074	0.021	>10	>10
SB590885	0.025	>10	>10
PLX4720	0.012	0.35	0.022

Several Raf inhibitors were evaluated against Raf-1 and A-Raf endogenously expressed in A375 cells and against recombinant Raf-1 in an in vitro phosphorylation assay. See also Figure S5, Table S5, and Table S6.

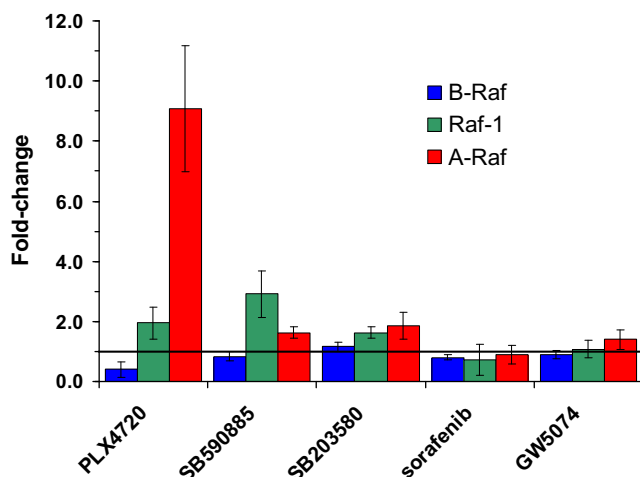


Figure 3. Cellular Properties of Raf Inhibitors

A375 cells were treated with the indicated inhibitors for 30 min. Cells were lysed, and the lysates analyzed using KiNativ. Data are plotted as the ratio of control versus treated signal for each indicated kinase. Error bars represent the range of duplicate data points. Data is representative of three separate duplicate experiments.

performed to date. The improvements to the KiNativ method achieved through the use of a targeted MS approach enable native kinase binding measurements to be made accurately and efficiently across >150 kinases in a single cell or tissue type. The method can be applied to any protein source, from any species, as long as DNA/protein sequence information is available. We demonstrate the capability to evaluate both Type I (DFG-in) and Type II (DFG-out) inhibitors and this method should be applicable to any kinase inhibitors that alter access of the probe to the ATP binding site. Through the global evaluation of ATP, staurosporine, and several clinical kinase inhibitors across >200 native kinases in two cell types (HL60 and PC3 cells), an intriguing picture of native kinase properties has emerged. Kinase biochemistry and drug development efforts have long relied on recombinant assays for characterization of kinase activity and inhibition and there are many examples of results that have been validated in vivo. However, protein kinases universally rely on protein-protein interactions for their function and are tightly regulated through multiple posttranslational mechanisms, often involving sequence regions distant from the protein kinase domain. Thus, it would be unreasonable to expect reconstituted in vitro assays, often using truncated kinase domain constructs, to provide an accurate assessment of in vivo properties in all cases. The global comparisons of native kinase binding properties determined here, with activity and binding assays of purified recombinant protein kinases demonstrated a clear correlation between binding/inhibition measurements supporting the general utility of recombinant kinase assays. However, the affinity of kinase inhibitors for their targets measured using the probe-based assay in cell lysates was often quite different from the respective values obtained using activity or binding assays of recombinant, isolated kinase preparations. These differences could be attributed to many possible factors including differences in the relative propensity of the assays to readout particular kinase conformations/activa-

tion states, differences in properties of full length versus truncated kinase constructs, and/or differences in the overall conformation of kinases in isolated systems versus the cellular milieu. Further work will be needed to determine the cause of these differences, and it is likely that multiple factors are at play. Nonetheless, the data shown here support the notion that inhibitor properties determined using the KiNativ assay are useful for predicting and interpreting the cellular behavior of kinase inhibitors.

No comprehensive data set of in vivo inhibitor potency against specific kinase phosphorylation events exists to allow for a global comparison with the profiles described here. However, the inhibitors discussed here have been the subject of detailed in vivo studies and their target potencies are well documented. For imatinib and dasatinib, the KiNativ assay results show excellent agreement with reported in vivo phosphorylation results against Abl and Src (Table 2). On the other hand, initial K_d^{app} measures for BIRB796 and erlotinib, were significantly weaker than some reported cellular EC_{50} values. Several studies have documented cellular potency of BIRB796 against p38 α in the low nM range (Pargellis et al., 2002; Kuma et al., 2005). However, BIRB796 is known to be a slow binder of p38 α , with maximal inhibition typically reached after 4 hr or more (Pargellis et al., 2002; Regan et al., 2003). Preincubations of BIRB796 with cell lysates for 4 hr showed a dramatic increase in potency (90% inhibition at 0.1 μ M, data not shown) to levels consistent with in vivo potency. Thus, the slow binding properties of BIRB796 likely account for the initial underestimate of p38 α potency.

Another somewhat surprising observation was the relatively weak affinity of erlotinib for EGFR. Recombinant assays typically suggest binding affinities in the low nM range (Gendreau et al., 2007), while we determined a K_d^{app} of 190 nM under our standard conditions. The initial K_d^{app} was measured in detergent-solubilized membranes from PC3 cells, which are known to have poor overall EGFR expression and are not used as models for EGFR-induced oncogenesis. The versatility of the KiNativ platform allowed for analysis of EGFR in an alternate cell line, MDA-MB-231, using both intact membranes and solubilized lysate preparations in either the resting state or after EGFR activation with EGF. Surprisingly, it was observed that the most significant shift in potency for erlotinib was found when comparing membrane bound versus detergent solubilized preparations. Erlotinib potency against EGFR in intact membranes was 5–10-fold stronger than in solubilized preparations. Importantly, when conditions of cellular efficacy studies were most closely mimicked, with EGFR on intact membranes after activation with EGF, the observed potency was consistent with the cellular potency. This result highlights the complex nature of small molecule-kinase interactions and demonstrates the value of a platform like KiNativ that enables the determination of binding constants for inhibitors against native kinases across any cell type of interest and using wide range of conditions.

Although it is not necessarily surprising that the inhibitory potency determined against kinases in a more native setting would more accurately reflect in vivo behavior of compounds, the striking correlation of the K_d^{app} values with in vivo potency found here is compelling (Tables 2–4). Several important factors distinguish the KiNativ assay from recombinant enzyme assays and may account for the discrepancies between recombinant

assays, the K_d^{app} , and the cellular efficacy. First, full length, endogenous enzymes are analyzed rather than the truncated and/or tagged forms often employed in recombinant enzyme assays. Differences in behavior between full length and truncated kinases have been noted previously (Donella-Deana et al., 1998). Second, the KiNativ IC_{50} values are a direct measure of active site binding rather than a measure of enzymatic activity. Thus, KiNativ is more a measure of the total pool of kinase capable of interacting with the ATP/ADP based probe, which may differ from the population of kinase capable of supporting activity in a specific assay. Third, the assay is performed under a setting more typical of a cellular environment with respect to the specific complement of proteins present and the overall protein concentrations. Thus, inhibitors may appear less potent due to decreased effective concentrations through either nonsaturable bulk protein affinity or the presence of high levels of specific targets. Fourth, posttranslational modifications and protein-protein interactions including kinase-substrate interactions, etc. are largely preserved in cell lysates. The precise conformation of the kinase active site, and/or steric accessibility of some binding sites will likely be affected by modifications and protein-protein interactions occurring in vivo and in cell lysates.

Although the data presented here support the trend that K_d^{app} accurately reflects the cellular pharmacological properties of the inhibitors examined, it is conceivable that this will not be true in all cases. For example, if a minor subpopulation of kinase is responsible for the majority of biological signaling, and a kinase inhibitor is selective for this particular kinase conformation, the KiNativ assay may not be able to detect the small change in signal that would result from inhibitor binding to this minor component. This potential issue highlights the complexity of kinase biology and the value of using multiple techniques to assess the pharmacological properties of kinase inhibitors. It is likely that no single kinase assay format will elucidate the relevant binding properties of inhibitors in every case.

Importantly, the results presented here were determined in the absence of cellular ATP (the samples were gel-filtered before labeling). Thus the affects of cellular ATP competition do not account for the differences observed between recombinant enzyme assay K_d values and the K_d^{app} values presented here. The fact that kinase inhibitors typically show a ≥ 10 -fold loss of potency in cellular and/or in vivo assays when compared to recombinant assays has commonly been attributed to competition with endogenous ATP (Knight and Shokat, 2005; Murphy et al., 2010). However, the data presented here suggest that even in the absence of ATP, most kinase inhibitors show reduced potency in a more native setting relative to recombinant enzyme assays. The fact that ATP is removed by gel-filtration before analysis and that the measured K_d^{app} is in excellent quantitative agreement with cellular efficacy in many cases, implies that competition with endogenous ATP may be only a minor issue for some kinases in vivo. All estimates of cellular ATP concentrations that we are aware of assess the aggregate, averaged ATP level in disrupted cellular material. It is very possible that this bulk ATP is highly compartmentalized such that many kinases may not experience ATP levels sufficient to cause dramatic competition with ATP site directed inhibitors. Nonetheless, it is noteworthy that the K_d^{app} appears to be an excellent

predictor of cellular efficacy, and this capability affords the KiNativ platform a unique capacity in kinase inhibitor drug discovery/development.

Although the relative trends of inhibition observed here agree reasonably well with recombinant assays, several outlying data points suggest more complex behavior for particular kinases. The three Raf kinase isoforms are a set of particularly interesting examples in this regard. Interestingly, the first clinically approved Raf kinase inhibitor, sorafenib, has more recently been shown to exert its activity through kinase targets other than Raf kinases (Smalley and Flaherty, 2009). Using the KiNativ platform, we discovered that native Raf kinases show a very different structure-activity relationship compared to their recombinant counterparts. Some compounds, such as PLX4720 and SB590885, show reasonably consistent potency between recombinant, KiNativ, and cellular/phenotypic assays whereas other compounds, such as sorafenib, GW5074, and SB203580, show dramatic differences. Importantly, for all of the compound classes, the K_d^{app} agrees very well with cellular phenotypic and in vivo phosphorylation data. Thus, the differences in behavior observed for these compounds between recombinant and cellular assays appear to be due to differences in the precise properties and/or conformation of the kinases in a native setting compared to the protein conformations expressed in isolated recombinant systems.

While exploring the behavior of Raf kinases, a second powerful property of the KiNativ platform became apparent. Recent literature reports have noted the ability of some Raf kinase inhibitors, namely SB203580 (Hall-Jackson et al., 1999a, 1999b), SB590885 (Heidorn et al., 2010), and PLX4720 (Hatzivassiliou et al., 2010; Poulikakos et al., 2010), to cause a paradoxical activation of Raf-1 in cellular settings. The analysis of cellular kinases after treatment with Raf inhibitors confirmed the ability of some Raf inhibitors to activate both Raf-1 and A-Raf. Recent literature has demonstrated that B-Raf can form hetero-complexes with both Raf-1 and A-Raf (Weber et al., 2001; Karreth et al., 2009). Further, it has been demonstrated that occupancy of the ATP site of a Raf kinase involved in a Raf-Raf dimer can cause trans-activation of the binding partner (Poulikakos et al., 2010). Two aspects of the data presented here are particularly interesting given this recent literature on the subject. First, PLX4720, which was the only compound found in our studies to be a functional inhibitor of A-Raf, also caused the most dramatic A-Raf activation on cellular treatment. Thus it appears likely that A-Raf transactivation occurs in a manner similar to what has been reported for B- and Raf-1. Furthermore, A-Raf transactivation may require direct binding to A-Raf, but may not occur efficiently through B-Raf or Raf-1 ATP site occupancy. Second, the data presented here clearly demonstrate that Raf transactivation occurs in A375 cells, which contain the V600E B-Raf mutation. In contrast, no reports to date have found any evidence of Raf transactivation in V600E-B-Raf melanoma lines based on p-ERK1/2, p-MAP2K1 levels and/or immunoprecipitation functional assays. Functional transactivation, manifested as increased p-MAP2K1/p-ERK1/2 levels, has only been observed in WT-B-Raf and WT-B-Raf/mutant-Ras containing cell lines. It has been hypothesized that this unusual observation results from decreased Ras expression in V600E-B-Raf expressing cells that would prevent the formation of Raf homo- and

hetero-dimers (Poulikakos et al., 2010). Our results show, however, that an aspect of transactivation, possibly a conformational change leading to increased ATP affinity, does occur even in V600E-B-Raf cellular background. Thus, Raf dimers likely exist in these cells and exhibit similar properties to their counterparts in WT-B-Raf backgrounds. The failure of the Raf molecular transactivation event to enhance ERK pathway signaling in V600E-B-Raf cells may be due to differences in cellular context not related to the presence/absence of Raf dimers (but possibly still related to Ras expression/activity). The ability of this platform to directly monitor conformational/activation events in kinase signaling pathways is a unique and powerful advantage for deciphering complex kinase biology.

Overall the platform detailed here provides a powerful tool to globally study the behavior of kinases in a nearly-intact cellular context. This platform enables quantitative assessment of nearly all protein and lipid kinases in any given cell or tissue type and permits determination of small molecule/kinase affinity for native enzymes with endogenous binding partners and post-translational modifications intact. The platform is also species independent as long as protein sequence information is available for the organism of interest. The specific data presented here provide the most complete picture of native kinase ATP and inhibitor specificity presented to date. From these data it is clear that cellular kinases are regulated through mechanisms that are not currently accounted for in recombinant assay systems. The KiNativ platform provides critical and relevant data to develop selective and potent kinase inhibitors and/or assess the in vivo function of kinases.

SIGNIFICANCE

Protein kinases are the largest and one of the most important enzyme families in mammals. The KiNativ platform described here is streamlined for global profiling of kinase ATP-binding sites directly in cell and tissue lysates. Binding constants for ATP, staurosporine, and five advanced or clinical-stage kinase inhibitors were determined in two different cell types. In general, the data support the known properties of kinase inhibitors, however, some striking differences from recombinant assay data were observed. In the Raf kinase family, the activity of inhibitors against recombinant Raf kinases were found to show almost no correlation with binding to native Raf kinases. For B-Raf signaling it was demonstrated that native kinase binding correlated very well with cellular inhibition of B-Raf signaling. This result demonstrates that kinases in their native environment can exist in distinct conformations that are not accurately represented in purified/recombinant kinase preparations. In several cases, inhibitor binding constants were found to closely match the EC₅₀ for cellular activity. This result suggests that the cellular ATP levels experienced by many protein kinases do not contribute significantly to the reduced levels of potency in the cellular setting. Many differences between inhibitor potency observed between recombinant kinase assays and cellular activity may be attributed simply to differences in the properties of the kinase targets in their native setting. These results have important implications for the design of kinase

targeted therapeutics and also highlight the importance of platforms like KiNativ that allow for detailed and comprehensive investigations of kinases in a native state.

EXPERIMENTAL PROCEDURES

ATP and ADP Acyl-Nucleotide Probes

ATP and ADP Acyl-nucleotide probes were synthesized as described previously except that desthiobiotin was substituted for biotin in all cases (Patricelli et al., 2007). Additional information regarding purification conditions, nuclear magnetic resonance data, etc. is located in the [Supplemental Experimental Procedures](#).

Lysate Preparation for Probe-Based Inhibitor Profiling

Cell pellets were resuspended in four volumes of lysis buffer (25 mM Tris pH 7.6, 150 mM NaCl, 1% CHAPS, 1% Tergitol NP-40 type, 1% v/v phosphatase inhibitor cocktail II [EMD/Calbiochem, #524625]), sonicated using a tip sonicator, and Dounce homogenized. Lysates were cleared by centrifugation at 100,000 × g for 30 min. The cleared lysates were filtered through a 0.22 μM syringe filter, and gel filtered (BioRad 10DG) into reaction buffer (20 mM HEPES pH 7.8, 150 mM NaCl, 0.1% Triton X-100, 1% v/v phosphatase inhibitor cocktail II [EMD/Calbiochem, #524625]). MnCl₂ was then added to the lysate to a final concentration of 20 mM before inhibitor treatment and probe labeling. Final inhibitor concentrations used for IC₅₀ determinations were 10, 1, 0.1, and 0.01 μM. ATP competition experiments were performed at 1000, 100, 10, and 1 μM ATP. All inhibitor treatments were performed at room temperature.

Recombinant Enzyme Samples

Recombinant ErbB2 (amino acids 679–1255) was obtained from Enzo Life Sciences. Wild-type B-Raf and V599E B-Raf (amino acids 416–766) were obtained from Invitrogen. Raf-1 (amino acids 1–149) was obtained from Millipore.

Preparation of Intact Membranes and Cellular Assay Conditions

Detailed information regarding membrane preparations and cellular assays is located in the [Supplemental Experimental Procedures](#).

Probe Labeling and Sample Preparation

Unless otherwise noted, all probe reactions were performed at room temperature with a final probe concentration of 5 μM after a 15 min preincubation of lysate with inhibitor. All reactions were performed in duplicate, using 445 μl/sample at 5 mg/ml. Samples were prepared for MS analysis essentially as described previously (Okerberg et al., 2005). Briefly, probe-labeled lysates were denatured and reduced (6 M urea, 10 mM DTT, 65°C, 15 min), alkylated (40 mM Iodoacetamide, 37°C, 30 min), and gel filtered (BioRad 10DG) into 10 mM ammonium bicarbonate, 2 M urea, 5 mM methionine. The desalted protein mixture was digested with trypsin (0.015 mg/ml) for 1 hr at 37°C, and desthiobiotinylated peptides captured using 12.5 μl high-capacity streptavidin resin (Thermo Scientific). Captured peptides were then washed extensively using 150 μl/wash with three different wash buffers: (A) 10 times with 1% triton, 0.5% tergitol, 1 mM EDTA in PBS; (B) 60 times with PBS; and (C) 15 times with HPLC grade water. Peptides were eluted from the streptavidin beads using two 35-μl washes of a 50% CH₃CN/water mixture containing 0.1% TFA at room temperature.

LC-MS/MS Analysis

Samples were analyzed by LC-MS/MS as described previously (Okerberg et al., 2005). Detailed information regarding data collection is located in the [Supplemental Experimental Procedures](#).

Data Analysis

All MS data were analyzed using custom software that was designed to extract and normalize signals from relevant probe-labeled peptides. Detailed information regarding this process is located in the [Supplemental Experimental Procedures](#).

Determination of K_d^{app} Values from KiNativ Determined IC_{50} Values

Detailed information regarding the determination of K_d^{app} is located in the Supplemental Experimental Procedures.

SUPPLEMENTAL INFORMATION

Supplemental Information includes Supplemental Experimental Procedures, seven figures, and six tables and can be found with this article online at doi:10.1016/j.chembiol.2011.04.011.

ACKNOWLEDGMENTS

M.P.P., T.K.N., J.W., H.B., D.Z., S.J., A.A., E.O., C.H., B.N., H.W., and J.W.K. are current or former employees of ActivX Biosciences, Inc.

Received: October 28, 2010

Revised: March 21, 2011

Accepted: April 4, 2011

Published: June 23, 2011

REFERENCES

- Bantscheff, M., Eberhard, D., Abraham, Y., Bastuck, S., Boesche, M., Hobson, S., Mathieson, T., Perrin, J., Raida, M., Rau, C., et al. (2007). Quantitative chemical proteomics reveals mechanisms of action of clinical ABL kinase inhibitors. *Nat. Biotechnol.* **25**, 1035–1044.
- Carey, K.D., Garton, A.J., Romero, M.S., Kahler, J., Thomson, S., Ross, S., Park, F., Haley, J.D., Gibson, N., and Sliwkowski, M.X. (2006). Kinetic analysis of epidermal growth factor receptor somatic mutant proteins shows increased sensitivity to the epidermal growth factor receptor tyrosine kinase inhibitor, erlotinib. *Cancer Res.* **66**, 8163–8171.
- Cohen, M.H., Williams, G., Johnson, J.R., Duan, J., Gobburu, J., Rahman, A., Benson, K., Leighton, J., Kim, S.K., Wood, R., et al. (2002). Approval summary for imatinib mesylate capsules in the treatment of chronic myelogenous leukemia. *Clin. Cancer Res.* **8**, 935–942.
- Cohen, P. (2002). Protein kinases—the major drug targets of the twenty-first century? *Nat. Rev. Drug Discov.* **1**, 309–315.
- Cuenda, A., Rouse, J., Doza, Y.N., Meier, R., Cohen, P., Gallagher, T.F., Young, P.R., and Lee, J.C. (1995). SB 203580 is a specific inhibitor of a MAP kinase homologue which is stimulated by cellular stresses and interleukin-1. *FEBS Lett.* **364**, 229–233.
- Domon, B., and Aebersold, R. (2010). Options and considerations when selecting a quantitative proteomics strategy. *Nat. Biotechnol.* **28**, 710–721.
- Donella-Deana, A., Cesaro, L., Ruzzene, M., Brunati, A.M., Marin, O., and Pinna, L.A. (1998). Spontaneous autophosphorylation of Lyn tyrosine kinase at both its activation segment and C-terminal tail confers altered substrate specificity. *Biochemistry* **37**, 1438–1446.
- Garcia-Echeverria, C., Traxler, P., and Evans, D.B. (2000). ATP site-directed competitive and irreversible inhibitors of protein kinases. *Med. Res. Rev.* **20**, 28–57.
- Garrington, T.P., and Johnson, G.L. (1999). Organization and regulation of mitogen-activated protein kinase signaling pathways. *Curr. Opin. Cell Biol.* **11**, 211–218.
- Gendreau, S.B., Ventura, R., Keast, P., Laird, A.D., Yakes, F.M., Zhang, W., Bentzien, F., Cancilla, B., Lutman, J., Chu, F., et al. (2007). Inhibition of the T790M gatekeeper mutant of the epidermal growth factor receptor by EXEL-7647. *Clin. Cancer Res.* **13**, 3713–3723.
- Godl, K., Wissing, J., Kurtenbach, A., Habenberger, P., Blencke, S., Gutbrod, H., Salassidis, K., Stein-Gerlach, M., Missio, A., Cotten, M., and Daub, H. (2003). An efficient proteomics method to identify the cellular targets of protein kinase inhibitors. *Proc. Natl. Acad. Sci. USA* **100**, 15434–15439.
- Hall-Jackson, C.A., Eyers, P.A., Cohen, P., Goedert, M., Boyle, F.T., Hewitt, N., Plant, H., and Hedge, P. (1999a). Paradoxical activation of Raf by a novel Raf inhibitor. *Chem. Biol.* **6**, 559–568.
- Hall-Jackson, C.A., Goedert, M., Hedge, P., and Cohen, P. (1999b). Effect of SB 203580 on the activity of c-Raf in vitro and in vivo. *Oncogene* **18**, 2047–2054.
- Hantschel, O., Rix, U., Schmidt, U., Burckstummer, T., Kneidinger, M., Schutze, G., Colinge, J., Bennett, K.L., Ellmeier, W., Valent, P., and Superti-Furga, G. (2007). The Btk tyrosine kinase is a major target of the Bcr-Abl inhibitor dasatinib. *Proc. Natl. Acad. Sci. USA* **104**, 13283–13288.
- Hatzivassiliou, G., Song, K., Yen, I., Brandhuber, B.J., Anderson, D.J., Alvarado, R., Ludlam, M.J., Stokoe, D., Gloor, S.L., Vigers, G., et al. (2010). RAF inhibitors prime wild-type RAF to activate the MAPK pathway and enhance growth. *Nature* **464**, 431–435.
- Heidorn, S.J., Milagre, C., Whittaker, S., Nourry, A., Niculescu-Duvas, I., Dhomen, N., Hussain, J., Reis-Filho, J.S., Springer, C.J., Pritchard, C., and Marais, R. (2010). Kinase-dead BRAF and oncogenic RAS cooperate to drive tumor progression through CRAF. *Cell* **140**, 209–221.
- Karaman, M.W., Herrgard, S., Treiber, D.K., Gallant, P., Atteridge, C.E., Campbell, B.T., Chan, K.W., Ciceri, P., Davis, M.L., Edeen, P.T., et al. (2008). A quantitative analysis of kinase inhibitor selectivity. *Nat. Biotechnol.* **26**, 127–132.
- Karreth, F.A., DeNicola, G.M., Winter, S.P., and Tuveson, D.A. (2009). C-Raf inhibits MAPK activation and transformation by B-Raf(V600E). *Mol. Cell* **36**, 477–486.
- Knight, Z.A., and Shokat, K.M. (2005). Features of selective kinase inhibitors. *Chem. Biol.* **12**, 621–637.
- Kuma, Y., Sabio, G., Bain, J., Shpiro, N., Marquez, R., and Cuenda, A. (2005). BIRB796 inhibits all p38 MAPK isoforms in vitro and in vivo. *J. Biol. Chem.* **280**, 19472–19479.
- Kupcho, K.R., Bruinsma, R., Hallis, T.M., Lasky, D.A., Somberg, R.L., Turek-Etienne, T., Vogel, K.W., and Huwiler, K.G. (2008). Fluorescent cascade and direct assays for characterization of RAF signaling pathway inhibitors. *Curr. Chem. Genomics* **1**, 43–53.
- Lackey, K., Cory, M., Davis, R., Frye, S.V., Harris, P.A., Hunter, R.N., Jung, D.K., McDonald, O.B., McNutt, R.W., Peel, M.R., et al. (2000). The discovery of potent cRaf1 kinase inhibitors. *Bioorg. Med. Chem. Lett.* **10**, 223–226.
- Leung, D., Hardouin, C., Boger, D.L., and Cravatt, B.F. (2003). Discovering potent and selective reversible inhibitors of enzymes in complex proteomes. *Nat. Biotechnol.* **21**, 687–691.
- Liu, Y., and Gray, N. (2006). Rational design of inhibitors that bind to inactive kinase conformations. *Nat. Chem. Biol.* **2**, 358–364.
- Manning, G., Whyte, D.B., Martinez, R., Hunter, T., and Sudarsanam, S. (2002). The protein kinase complement of the human genome. *Science* **298**, 1912–1934.
- Murphy, E.A., Shields, D.J., Stoletov, K., Dneprovskaja, E., McElroy, M., Greenberg, J.I., Lindquist, J., Acevedo, L.M., Anand, S., Majeti, B.K., et al. (2010). Disruption of angiogenesis and tumor growth with an orally active drug that stabilizes the inactive state of PDGFRbeta/B-RAF. *Proc. Natl. Acad. Sci. USA* **107**, 4299–4304.
- Newton, A.C. (2001). Protein kinase C: structural and spatial regulation by phosphorylation, cofactors, and macromolecular interactions. *Chem. Rev.* **101**, 2353–2364.
- Noble, M.E., Endicott, J.A., and Johnson, L.N. (2004). Protein kinase inhibitors: insights into drug design from structure. *Science* **303**, 1800–1805.
- Okerberg, E.S., Wu, J., Zhang, B., Samii, B., Blackford, K., Winn, D.T., Shreder, K.R., Burbaum, J.J., and Patricelli, M.P. (2005). High-resolution functional proteomics by active-site peptide profiling. *Proc. Natl. Acad. Sci. USA* **102**, 4996–5001.
- Pargellis, C., Tong, L., Churchill, L., Cirillo, P.F., Gilmore, T., Graham, A.G., Grob, P.M., Hickey, E.R., Moss, N., Pav, S., and Regan, J. (2002). Inhibition of p38 MAP kinase by utilizing a novel allosteric binding site. *Nat. Struct. Biol.* **9**, 268–272.
- Patricelli, M.P., Szardenings, A.K., Liyanage, M., Nomanbhoy, T.K., Wu, M., Weissig, H., Aban, A., Chun, D., Tanner, S., and Kozarich, J.W. (2007). Functional interrogation of the kinome using nucleotide acyl phosphates. *Biochemistry* **46**, 350–358.

- Poulikakos, P.I., Zhang, C., Bollag, G., Shokat, K.M., and Rosen, N. (2010). RAF inhibitors transactivate RAF dimers and ERK signalling in cells with wild-type BRAF. *Nature* *464*, 427–430.
- Regan, J., Pargellis, C.A., Cirillo, P.F., Gilmore, T., Hickey, E.R., Peet, G.W., Proto, A., Swinamer, A., and Moss, N. (2003). The kinetics of binding to p38MAP kinase by analogues of BIRB 796. *Bioorg. Med. Chem. Lett.* *13*, 3101–3104.
- Schiffer, H.H., Reding, E.C., Fuhs, S.R., Lu, Q., Piu, F., Wong, S., Littler, P.L., Weiner, D.M., Keefe, W., Tan, P.K., et al. (2007). Pharmacology and signaling properties of epidermal growth factor receptor isoforms studied by bioluminescence resonance energy transfer. *Mol. Pharmacol.* *71*, 508–518.
- Schmidt, A., Claassen, M., and Aebersold, R. (2009). Directed mass spectrometry: towards hypothesis-driven proteomics. *Curr. Opin. Chem. Biol.* *13*, 510–517.
- Sharma, K., Weber, C., Bairlein, M., Greff, Z., Kéri, G., Cox, J., Olsen, J.V., and Daub, H. (2009). Proteomics strategy for quantitative interaction profiling in cell extracts. *Nat. Methods* *6*, 741–744.
- Smalley, K.S., and Flaherty, K.T. (2009). Development of a novel chemical class of BRAF inhibitors offers new hope for melanoma treatment. *Future Oncol.* *5*, 775–778.
- Takle, A.K., Brown, M.J., Davies, S., Dean, D.K., Francis, G., Gaiba, A., Hird, A.W., King, F.D., Lovell, P.J., Naylor, A., et al. (2006). The identification of potent and selective imidazole-based inhibitors of B-Raf kinase. *Bioorg. Med. Chem. Lett.* *16*, 378–381.
- Toledo, L.M., Lydon, N.B., and Elbaum, D. (1999). The structure-based design of ATP-site directed protein kinase inhibitors. *Curr. Med. Chem.* *6*, 775–805.
- Tsai, J., Lee, J.T., Wang, W., Zhang, J., Cho, H., Mamo, S., Bremer, R., Gillette, S., Kong, J., Haass, N.K., et al. (2008). Discovery of a selective inhibitor of oncogenic B-Raf kinase with potent antimelanoma activity. *Proc. Natl. Acad. Sci. USA* *105*, 3041–3046.
- Weber, C.K., Slupsky, J.R., Kalmes, H.A., and Rapp, U.R. (2001). Active Ras induces heterodimerization of cRaf and BRaf. *Cancer Res.* *61*, 3595–3598.
- Wilhelm, S.M., Carter, C., Tang, L., Wilkie, D., McNabola, A., Rong, H., Chen, C., Zhang, X., Vincent, P., McHugh, M., et al. (2004). BAY 43-9006 exhibits broad spectrum oral antitumor activity and targets the RAF/MEK/ERK pathway and receptor tyrosine kinases involved in tumor progression and angiogenesis. *Cancer Res.* *64*, 7099–7109.
- Winkler, J.D., Sarau, H.M., Foley, J.J., and Crooke, S.T. (1988). Phorbol 12-myristate 13-acetate inhibition of leukotriene D4-induced signal transduction was rapidly reversed by staurosporine. *Biochem. Biophys. Res. Commun.* *157*, 521–529.